Research Article | Vol. 7, No. 11 | 1 Nov 2017 | OPTICAL MATERIALS EXPRESS 3815
Optical Materials EXPRESS

Thermo-optical and lasing characteristics of Cr^{2+}-doped CdSe single crystal as tunable coherent source in the mid-infrared

TONEY T. FERNANDEZ,[1] MIKHAIL K. TARABRIN,[2,3] YUCHEN WANG,[1] VLADIMIR A. LAZAREV,[2] STANISLAV O. LEONOV,[2] VALERIY E. KARASIK,[2] YURII V. KOROSTELIN,[3] MIKHAIL P. FROLOV,[3,4] YURII P. PODMARKOV,[3] YAN K. SKASYRSKY,[3] VLADIMIR I. KOZLOVSKY,[3,5] CESARE SVELTO,[6] PASQUALE MADDALONI,[7] NICOLA COLUCCELLI,[1,8] PAOLO LAPORTA,[1,8] AND GIANLUCA GALZERANO[1,8,*]

[1]*Dipartimento di Fisica - Politecnico di Milano, Piazza Leonardo da Vinci 32, 20133 Milano, Italy*
[2]*Bauman Moscow State Technical University, Moscow 105005, Russia*
[3]*P. N. Lebedev Physical Institute of the Russian Academy of Sciences, Moscow 119991, Russia*
[4]*Moscow Institute of Physics and Technology, Moscow 117303, Russia*
[5]*National Research Nuclear University MEPhI, Moscow 115409, Russia*
[6]*Dipartimento di Elettronica, Informazione e Bioingegneria - Politecnico di Milano, Via Ponzio 34/5, 20133 Milan, Italy*
[7]*Istituto Nazionale di Ottica - Consiglio Nazionale delle Ricerche, Via Campi Flegrei 34, 80078 Pozzuoli (NA), Italy*
[8]*Istituto di Fotonica e Nanotecnologie - Consiglio Nazionale delle Ricerche, Piazza Leonardo da Vinci 32, 20133 Milano, Italy*
[*]*gianluca.galzerano@polimi.it*

Abstract: We report on a comprehensive characterization of Cr^{2+}-doped CdSe single crystal as an efficient active material for tunable laser applications in the mid-infrared spectral region. Optical gain, thermo-optical behavior, power efficiency, scalability and wavelength tunability have been thoroughly investigated. Using an antireflection-coated crystal pumped by a Tm-fiber laser at at 1.94 μm, 1-W CW output power and 50% slope efficiency at 2.65 μm emission wavelength have been obtained in a diffraction-limited output beam. An output peak power of 2.5 W has been achieved without significant beam distortion in a quasi-CW regime. Exploiting an intra-cavity diffraction grating in a Littrow configuration, a maximum tuning range of 900 nm from 2.22 to 3.12 μm, limited by the finite bandwidth of resonator components, has been demonstrated with an uncoated crystal.

OCIS codes: (140.5680) Rare earth and transition metal solid-state lasers; (140.3070) Infrared and far-infrared lasers; (160.6990) Transition-metal-doped materials.

References and links

1. V. Kasiyan, R. Shneck, Z. Dashevsky, and S. Rotman, "Development of $A^{II}B^{VI}$ semiconductors doped with Cr for IR laser application," Physica Status Solidi (b) **229**, 395–398 (2002).
2. I. T. Sorokina, "Cr^{2+}-doped II-VI materials for lasers and nonlinear optics," Opt. Mater. **26**, 395 – 412 (2004).
3. S. Mirov, V. Fedorov, I. Moskalev, M. Mirov, and D. Martyshkin, "Frontiers of mid-infrared lasers based on transition metal doped II-VI semiconductors," J. Luminesc. **133**, 268 – 275 (2013).
4. S. Mirov, V. Fedorov, D. Martyshkin, I. Moskalev, M. Mirov, and S. Vasilyev, "Progress in Mid-IR lasers based on Cr and Fe-Doped II-VI chalcogenides," IEEE J. Sel. Top. Quantum Electron. **21**, 292–310 (2015).
5. K. Schepler, S. Kück, and L. Shiozawa, "Emission spectroscopy in CdSe," J. Luminesc. **72-74**, 116 – 117 (1997).
6. J. McKay, K. L. Schepler, and G. C. Catella, "Efficient grating-tuned mid-infrared Cr^{2+} : CdSe laser," Opt. Lett. **24**, 1575–1577 (1999).
7. J. McKay, K. L. Schepler, and G. Catella, "Kilohertz, 2.6-μm Cr^{2+} : CdSe laser," in "Advanced Solid State Lasers," (Optical Society of America, 1999), p. WD1.

#302888 https://doi.org/10.1364/OME.7.003815
Journal © 2017 Received 19 Jul 2017; revised 18 Sep 2017; accepted 19 Sep 2017; published 3 Oct 2017

8. V. Kasiyan, Z. Dashevsky, R. Shneck, and S. Rotman, "Novel lasing materials based on CdSe crystals doped with Cr," Proc. SPIE **5123**, 79–84 (2003).
9. V. A. Akimov, V. I. Kozlovskii, Y. V. Korostelin, A. I. Landman, Y. P. Podmar'kov, Y. K. Skasyrsky, and M. P. Frolov, "Efficient cw lasing in a Cr^{2+} : CdSe crystal," Quant. Electron. **37**, 991 (2007).
10. V. I. Kozlovskii, Y. V. Korostelin, A. I. Landman, Y. P. Podmar'kov, Y. K. Skasyrsky, and M. P. Frolov, "Continuous-wave Cr^{2+} : CdS laser," Quant. Electron. **40**, 7 (2010).
11. V. A. Akimov, V. I. Kozlovskii, Y. V. Korostelin, A. I. Landman, Y. P. Podmar'kov, Y. K. Skasyrskii, and M. P. Frolov, "Efficient pulsed Cr^{2+} : CdSe laser continuously tunable in the spectral range from 2.26 to 3.61 μm," Quant. Electron. **38**, 205 (2008).
12. M. A. Gubin, A. N. Kireev, Yu. V. Korostelin, A. I. Landman, Yu. P. Podmarkov, M. Yu. Filipchuk, M. P. Frolov, A. I. and Shelkovnikov, "Tunable single-frequency CW Cr^{2+}:CdSe laser," Bull. Lebedev Phys. Inst. **38**, 205 (2011).
13. O. L. Antipov, I. D. Eranov, M. P. Frolov, Yu V. Korostelin, V. I. Kozlovsky, A. A. Novikov, Yu P. Podmarkov, and Ya K. Skasyrsky, "2.92 μm Cr^{2+}:CdSe single crystal laser pumped by a repetitively pulsed Tm^{3+}:Lu_2O_3 ceramics laser at 2.066 μm," Laser Phys. Lett. **4**, 045801, (2015).
14. V. A. Lazarev, M. K. Tarabrin, A. A. Kovtun, V. E. Karasik, A. N. Kireev, V. I. Kozlovsky, Yu V. Korostelin, Yu P. Podmarkov, M. P. Frolov, and M. A. Gubin, "Continuous-wave broadly tunable diode laser array-pumped mid-infrared Cr^{2+}:CdSe laser," Laser Phys. Lett. **12**, 125003 (2015).
15. M. K. Tarabrin, A. Kovtun, V. Lazarev, V. Karasik, A. Kireev, V. Kozlovsky, Y. Korostelin, Y. Podmar'kov, M. Frolov, and M. Gubin, "Tunable CW Solid-State Mid-IR Cr^{2+}:CdSe Single Crystal Laser with Diode Laser Array Pumping," in Advanced Solid State Lasers, OSA Technical Digest (online) (Optical Society of America, 2015), paper AM5A.34.
16. V. A. Akimov, M. P. Frolov, Y. V. Korostelin, V. I. Kozlovsky, A. I. Landman, Y. P. Podmar'kov, and A. A. Voronov, "Vapour growth of II-VI single crystals doped by transition metals for mid-infrared lasers," Physica Status Solidi (c) **3**, 1213–1216 (2006).
17. O. Svelto, *Principles of Lasers*, 5th ed. (Springer, 2010).
18. K. L. Schepler, R. D. Peterson, P. A. Berry, and J. B. McKay, "Thermal Effects in Cr^{2+}:ZnSe Thin Disk Lasers," IEEE J. Sel. Top. Quant. Electron. **11**, 713–720 (2005).
19. Laser Cavity Design software, LASCAD^{TM}, *http://www.las-cad.com*.
20. N. E. Dowling, *Mechanical Behavior of Materials: Engineering Methods for Formation, Fracture, and Fatigue* (Prentice Hall, 1999).
21. W. Koechner, *Solid-state Laser Engineering*, 5th Ed. (Springer, 1999).
22. ISO Standard 11146, "Lasers and laser-related equipment – Test methods for laser beam widths, divergence angles and beam propagation ratios" (2005).
23. I. Moskalev, S. Mirov, M. Mirov, S. Vasilyev, V. Smolski, A. Zakrevskiy, and V. Gapontsev, "140 W Cr:ZnSe laser system," Opt. Express **24**, 21090–21104 (2016).
24. E. Deligoz, K. Colakoglu, and Y. Ciftci, "Elastic, electronic, and lattice dynamical properties of CdS, CdSe, and CdTe," Physica B **373**, 124–130 (2006).
25. J. Yang, H. Tang, Y. Zhao, Y. Zhang, J. Li, Z. Ni, Y. Chena, and D. Xu, "Thermal conductivity of zinc blende and wurtzite CdSe nanostructures," Nanoscale **7**, 16071–16078 (2015).

1. Introduction

Efficient and broad-emission-bandwidth coherent light sources in the middle-infrared (mid-IR) spectral region from 2 to 4 μm are of great interest for various applications in the fields of molecular spectroscopy, frequency metrology, industrial material processing, laser surgery, and optical radar systems for atmospheric remote sensing. Direct light generation in mid-IR region is usually achieved using hetero-junction lead-salt compounds, gallium-antimonide, or quantum- and interband-cascade semiconductor lasers. In most cases, however, these devices feature low output power, limited tuning range, and poor spatial beam quality. Optically-pumped transition-metal or rare-earth doped crystals provide another viable route for efficient generation of mid-IR light. In particular, Cr^{2+}-doped binary (*e.g.*, ZnSe, ZnS, CdSe, CdS, ZnTe) and ternary (*e.g.*, CdMnTe, CdZnTe, ZnSSe) chalcogenide crystals, having gain bandwidths up to 50% of the central wavelength, represent a class of solid-state gain media with ultra-broad absorption and emission bands with high cross-sections in the mid-IR range of optical spectrum [1–4]. Among the different chalcogenide crystals, Cr^{2+}:CdSe is a promising candidate, as its vibronic emission covers the 2.2–3.6 μm spectral range [5–8], which overlaps the fundamental vibrational transitions of hydrocarbons, water, and other relevant chemical and biological molecules. After the first laser actions in Cr:CdSe crystal [6,7], subsequent demonstrations proved excellent laser

Optical Materials EXPRESS

efficiencies and wide wavelength tunability both in continuous wave (CW) [9, 10] and in gain-switching regimes, using different pump sources such as Tm-doped crystal lasers, diode lasers, and Tm-fiber lasers [9–15]. However, attempts to develop Cr^{2+}:CdSe lasers with higher output power levels have been hampered by the strong sensitivity of CdSe crystal to thermo-optical effects, such as thermal lensing and mode wavefront distortion.

In this paper, we report on a comprehensive experimental investigation of Cr^{2+}-doped CdSe crystal in the mid-IR spectral region around 2.7 μm. Particular attention is devoted to the characterization of the main physical and technical limitations to power scalability and wavelength tunability of Tm-fiber-laser pumped Cr^{2+}:CdSe mono-crystal. Using an anti-reflection (AR) coated Cr^{2+}:CdSe crystal we demonstrated a diffraction-limited beam with a maximum CW output power of 1 W at the emission wavelength of 2.65 μm with an incident pump power of 2.1 W. This corresponds to a slope efficiency of 50% (63% with respect to the absorbed pump power) which, to the best of our knowledge, is the highest efficiency achieved in Cr:CdSe CW lasers. With the aim of assessing power scalability, we also investigated the thermal effects in Cr:CdSe crystal both in CW and in quasi-CW pumping regimes. We were able to increase the peak output power from 1 W to 2.5 W adopting a quasi-CW pumping without significant distortions of the laser mode. Using an uncoated Cr:CdSe crystal combined with a reflective diffraction grating in a Littrow configuration, a remarkable tuning range from 2.2 to 3.12 μm, limited only by the spectral bandwdith of the resonator elements (mirrors and grating), has been obtained. The full characterization of laser performance shows that Cr^{2+}:CdSe has the potential to be used as an efficient laser material for a variety of applications requiring low to medium output power levels (up to few watts) in the molecular fingerprint spectral region from 2800 to 4550 cm^{-1}.

2. Cr^{2+}-doped CdSe laser crystal

CdSe binary chalcogenide (II–VI semiconductor) crystal has hexagonal symmetry (C_{3v} space-group) with lattice parameters a=0.430 nm and c=0.702 nm. In our experiment, the CdSe mono-crystal was grown and simultaneously doped with Cr^{2+} ions using physical vapor phase transport deposition on a single-crystal seed (see ref. [16] for further details). Figure 1 (a) shows the absorption spectrum of the Cr^{2+}:CdSe crystal as retrieved from the measurement of the transmission spectrum. The absorption spectrum is characterized by a 430-nm broad (full width at half maximum) profile with a peak value of 3.32 cm^{-1} (corresponding to a Cr^{2+} doping level of $1.7 \cdot 10^{18}$ ions/cm^3 [3]) located at 1920-nm wavelength, which can be exploited for efficient

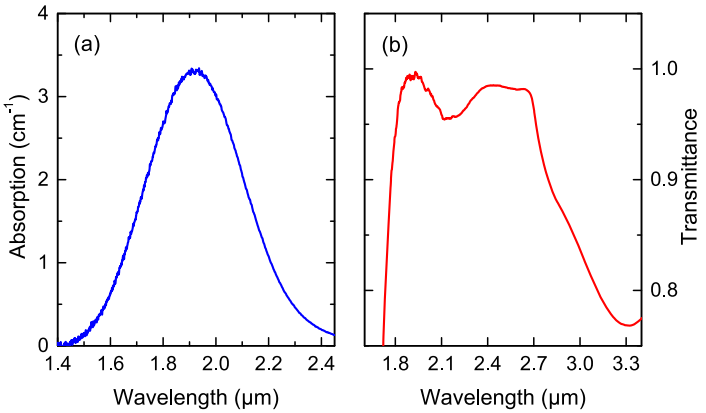

Fig. 1. (a) Absorption and (b) AR-coating transmission spectrum of the Cr^{2+}:CdSe crystal.

Optical Materials EXPRESS

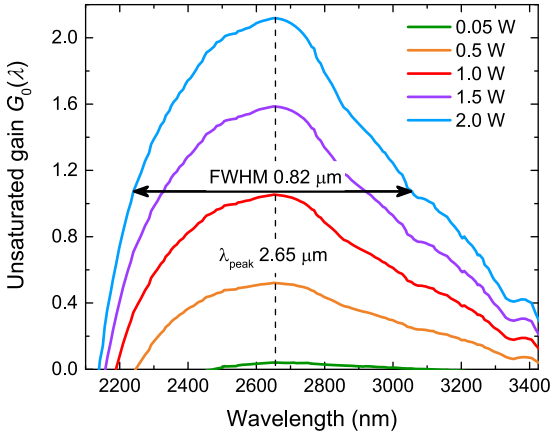

Fig. 2. Unsaturated round-trip gain of the Cr^{2+}:CdSe crystal as a function of emission wavelength for different values of the pump powers (η_p=0.73, η_a=0.8, τ=3.8 μs, w_l=55 μm, w_p=38 μm, N_t=1.7·10^{18} ions/cm^3, and l=4.9 mm).

pumping either by a Tm-fiber laser or a diode laser. In particular, the absorption coefficient at 1940 nm, corresponding to the peak emission wavelength of Tm-fiber laser, turns out to be 3.29 cm^{-1}. The Cr:CdSe crystal consists of a parallelepiped with 4.6 mm × 4.9 mm parallel facets (wedging less than 30″) and 4.9 mm length, leading to a pump absorption of ~80% at 1940 nm. Both facets were polished and anti-reflection (AR) coated for normal incidence using 10 Ta_2O_5/SiO_2 alternate layers (total coating thickness of 3.1 μm). Measured transmission curve for the single broad-band AR-coating of the crystal facet is shown in Fig. 1 (b). At the pump wavelength of 1940 nm, the transmission of the AR-coating is 0.996 and in the wavelength range from 1.77 to 2.79 μm it is higher than 0.9.

From the absorption and emission cross sections it is possible to evaluate the unsaturated round-trip linear gain of the Cr^{2+}:CdSe crystal using the following expression [17]:

$$G_0(\lambda) = \frac{4\eta_p\eta_a\tau}{\pi(w_l^2 + w_p^2)}\frac{P_p}{h\nu_p}\sigma_e(\lambda) - 2lN_t\sigma_a(\lambda) \quad (1)$$

where η_p is the pump quantum efficiency, η_a is the fraction of the incident pump power absorbed by the crystal, τ is the radiative lifetime of the emitting level, P_p is the incident pump power, λ is the wavelength, w_l and w_p are the laser and pump beam waists, respectively, h is Planck's constant, ν_p is the pump laser frequency, $\sigma_e(\lambda)$ and $\sigma_a(\lambda)$ are the emission and absorption cross sections, respectively, N_t is the Cr^{2+} concentration, and l is the crystal length; the negative contribution to the laser gain $2lN_t\sigma_a(\lambda)$ is due to reabsorption losses. Figures 2 depicts the laser gain as a function of wavelength for different values of the pump power, allowing to predict the tunability range of the laser for given pump power levels and for total round-trip linear losses $\delta(\lambda) = \delta_c + \delta_i$ (δ_c, transmission of the output coupler; δ_i, internal round-trip losses). Indeed, laser action is possible for each wavelength where the unsaturated laser gain exceeds the round trip losses, i.e. $G_0(\lambda) \geq \delta(\lambda)$. In particular, Fig. 2 shows that the laser gain begins to be positive for pump power as low as 50 mW and it is characterized by a peak at 2.65 μm, whose location remains unchanged even for increasing pump powers. By contrast, it is worth noting that the gain bandwidth broadens at increasing pump powers up to 0.82 μm at 2 W pump power level (full-width at half-maximum from 2.24 to 3.06 μm), demonstrating the ultra-broad emission potentiality of the Cr:CdSe. For example, assuming a constant intracavity total losses of 0.2 and a 2-W pump power level, a wavelength tunability from 2.15 to 3.45 μm is expected.

Optical Materials EXPRESS

Table 1. Main spectroscopic and thermo-optical properties of different chalcogenide crystals.

	ZnS [3,18]	ZnSe [3,18]	CdSe [3,18,24,25]
peak absorption cross section, σ_a (10^{-18} cm^2)	1.0	1.1	1.9
absorption peak wavelength, λ_a (μm)	1.69	1.77	1.89
peak emission cross section, σ_e (10^{-18} cm^2)	1.4	1.3	2.0
emission peak wavelength, λ_e (μm)	2.35	2.45	2.65
emission full width at half maximum, $\Delta\lambda_e$ (μm)	0.82	0.86	0.94
radiative lifetime at 290 K, τ (μs)	4.4	5.2	3.8
refractive index at λ=3 μm, n	2.26	2.44	2.50
thermal conductivity, k (WK^{-1}m^{-1})	27	19	9
Young's modulus, E (GPa),	74.5	67.2	61.2
Poisson ratio, ν	0.28	0.28	0.345
Knoop hardness, (kg mm^{-2})	178	100	44–90
fracture toughness, (MPa m$^{1/2}$)	0.86	0.50	0.27
temperature dependence of refractive index, dn/dT (10^{-6} K^{-1})	43	63	100
thermal linear expansion, α (10^{-6} K^{-1})	6.5	7.1	6.3
Figures of merit			
thermal shock parameter, $R_T = k(1-\nu)\sigma_T/(\alpha E)$ (Wm$^{-1/2}$)	34.5	14.3	4.1
thermal lensing factor, $K_T = (dn/dT)/k$ (10^{-6} mW^{-1})	1.6	3.3	11.1

In addition to the broad-band capability, a further important laser property is its power scalability, which is essentially limited by the thermomechanical properties of the active medium such as thermal conductivity (k), temperature dependence of refractive index (dn/dT), thermal linear expansion (α), and material fracture toughness (σ_T). To compare the power scalability of different active crystals two figures of merit are commonly adopted: the thermal shock parameter (R_T) and the thermal lensing factor (K_T) [18]. The thermal shock parameter, $R_T = k(1-\nu)\sigma_T/(\alpha E)$, where ν is the Poisson ratio and E is the Young's modulus, is used to express the material resistance to cracking under thermal load, whereas the thermal lensing factor, $K_T = (dn/dT)/k$, defines the thermal lens dioptric power, $DP_T = 1/f_T = I_p K_T$, due to temperature gradient inside the pumped laser crystal, being I_p the pump intensity (uniform pumping is assumed). Table 1 summarizes the main spectroscopic and thermo-optical properties of the CdSe crystal in comparison to those of the most investigated ZnS and ZnSe active media. Based on the values shown in Table 1, it appears that thermal lensing in CdSe is 7 and ~3.5 times stronger than in ZnS and ZnSe, respectively, and the thermal shock is 8 and ~3.5 times lower than in ZnS and ZnSe. Therefore, with respect to ZnS and ZnSe active media, thermal management is expected to be a significant issue in designing multiwatt class lasers based on Cr^{2+}:CdSe crystals, because both thermally induced optical distortion and thermal fracture effects must be closely considered. As an example, Fig. 3 shows a finite element analysis computation (FEA [19]) of the temperature and stress inside the investigated 4.9-mm thick Cr:CdSe crystal for a Gaussian pump beam with an incident pump power of 2 W and a spot size of 38 μm, corresponding to a pump intensity of ~0.8 GWm^{-2}. Although the maximum temperature increase in the CdSe crystal is limited to ~20 K with respect to the 290-K reference temperature of the bottom crystal surface, due to the large thermal lensing factor a thermal focal length as short as 1 mm is obtained. Concerning the calculated stress, FEA simulation yields a maximum intensity of $2 \cdot 10^6$ Nm^{-2} of the equivalent von-Mises stress [20] over a maximum length of 1.5 mm. This analysis reveals that for pump intensities approaching 1 GWm^{-2}, the power scalability of Cr:CdSe crystal is mainly limited by thermal lensing and optical beam distortion, being the thermal fracture issue well below the threshold value.

Optical Materials EXPRESS

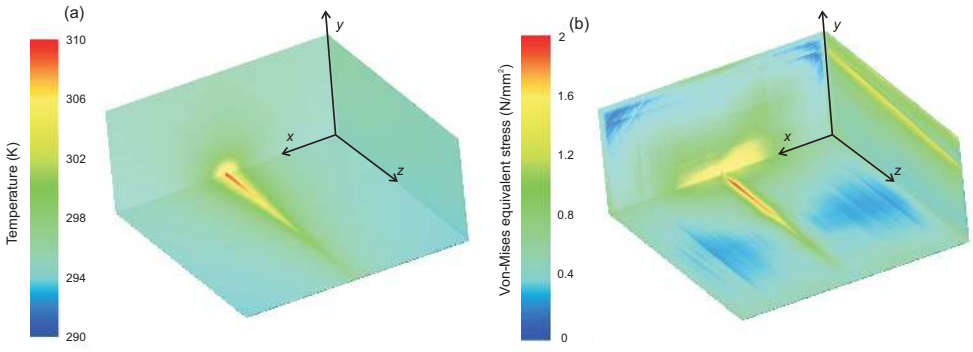

Fig. 3. (a) Temperature and (b) von-Mises equivalent stress profiles retrieved by a finite element analysis for a Gaussian pump beam with 2 W power and 38 μm spot size.

3. Cr^{2+}:CdSe laser experiment

3.1. High-efficiency CW laser action

Figure 4 (a) shows the experimental setup of the CW Cr^{2+}:CdSe laser. The linear resonator consists of a dichroic plane mirror (reflectance R >99.5% from 2350 to 3050 nm and transmittance T >95% at 1940 nm), a plano-concave folding mirror (R > 99.5% from 2100 to 3000 nm) with a radius of curvature of 100 mm, and a plane output coupler. The spherical mirror folds the resonator axis with a full angle of 8° and the total resonator length is 155 mm, whereas the distance between the plane dichroic and the spherical folding mirror is set to ≈53.7 mm. This resonator configuration provides a mode spot size (radius) of 61 μm × 54 μm inside the gain crystal as calculated by numerical simulations. The 4.9-mm thick AR-coated Cr:CdSe monocrystal is mounted on a copper heat sink kept at a constant temperature of 20 °C by a Peltier electric-cooler. The pump source is a CW single-transverse mode Tm:fiber laser (IPG Photonics, model TLR-LP-20) with a maximum output power of 20 W and a linearly polarized emission at 1.94 μm. The pump radiation is focused through the dichroic pump mirror into the Cr:CdSe crystal (38 μm spot size), using an AR-coated plano-convex lens with a focal length of 75 mm.

The performance of the CW Cr:CdSe laser was characterized in terms of output power versus incident pump power for different output coupler (OC) transmission values of 1.5%, 2%, 10%, and 20%. An external dichroic pump mirror was used to separate the residual pump power at 1.94 μm from the Cr:CdSe laser output power. In all cases the free-running emission wavelength

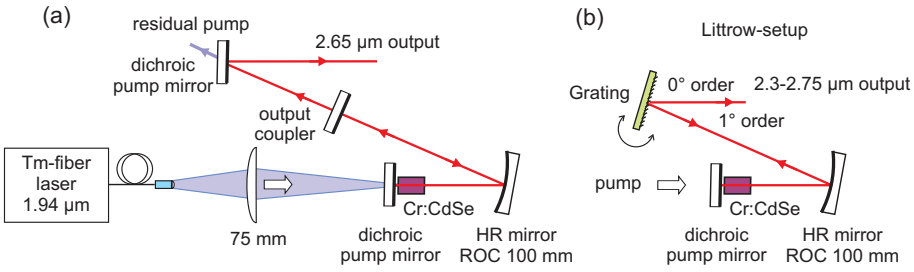

Fig. 4. Experimental setup for the Cr:CdSe laser: (a) folded three-mirror linear resonator; (b) Littrow-configuration for wavelength tunability characterization.

Optical Materials EXPRESS

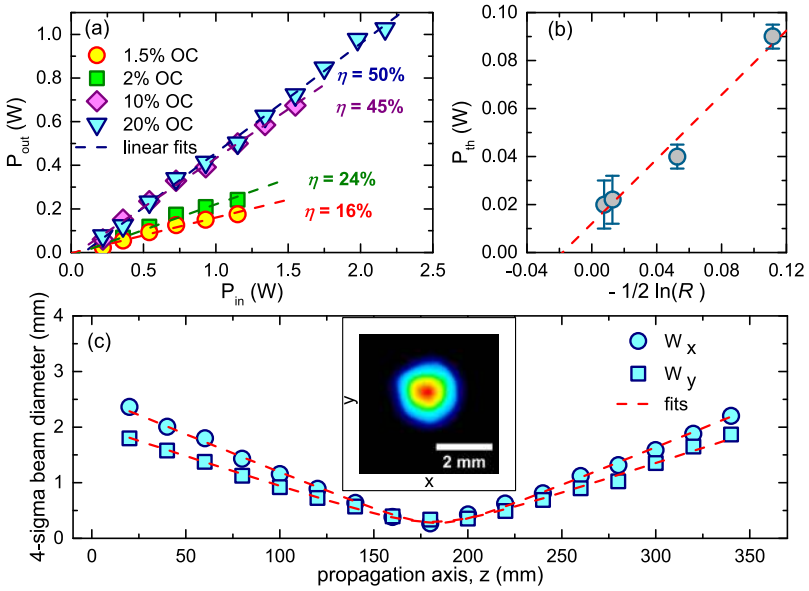

Fig. 5. (a) Cr:CdSe laser output power as a function of incident pump power for different output couplings. The dashed curves correspond to linear fits of the experimental data. (b) Measured threshold pump power as a function of the output coupling losses ($-\ln\sqrt{R}$).The dashed curve corresponds to a linear interpolation of the data. (c) Beam diameters (4-sigma) of the Cr:CdSe laser at 1-W output power versus the propagation distance (caustic curve) after a plano-convex lens with a focal length of 175 mm. Red dashed curves represent the best interpolation corresponding to the retrieved following parameters: M_x^2=1.1(1), W_{0x}=277(30) μm, z_{0x}=184(1) μm; M_y^2=1.0(1), W_{0y}=296(28) μm, z_{0y}=181(1) mm. Inset: 2D spatial beam profile recorded at z=340 mm, W_x=2200 μm and W_y=1866 μm.

of the laser is coincident with the Cr:CdSe emission peak at 2.65 μm. Figure 5 (a) shows the measured output versus input power characteristics. The best result in terms of output power and slope efficiency was obtained for the highest available 20% output coupling, with a maximum slope efficiency of 50%, corresponding to 63% efficiency with respect to the absorbed pump power, and a maximum output power of 1 W at the incident pump power level of 2.1 W (optical-to-optical efficiency of 48%). The pump power level was limited to ~2 W (see paragraph 3.3) to avoid output power and mode-beam instabilities due to the thermal load on the crystal. Lower efficiencies and output powers were achieved with the lower output couplings. The laser gain and the intracavity losses are retrieved by a Findlay-Clay analysis [21]. Figure 5 (b) shows the measured pump power thresholds versus the output coupling losses (corresponding to $-\ln\sqrt{R}$, where R is the output coupler reflectivity) together with the Findlay-Clay interpolating linear curve, $P_{th} = K(-\ln(\sqrt{R}) + \delta)$, where K is a coefficient related to the saturation intensity of the laser transition as well as to the quantum and pump efficiencies, and δ is the intracavity logarithmic loss taking into account also the mirrors reflectivity. The best interpolation of the experimental data reported in Fig. 5 (b) yields $\delta = 0.02(1)$ and $K = 0.67(7)$ W.

At the 1-W output power level, the spatial quality of the laser beam at 2.65 μm was characterized using a mid-infrared camera (DataRay Inc, model WinCamD-FIR2-16-HR). To properly measure the M^2 beam quality factor, the nearly collimated output beam of the Cr:CdSe laser is focused by means of a plano-convex lens with 175-mm focal length, and the 4-sigma diameters are measured at different propagation distances in accordance to the ISO 11146 standard [22]. Figure 5 (c) shows the measured 4-sigma diameters along the transverse x- and

Optical Materials EXPRESS

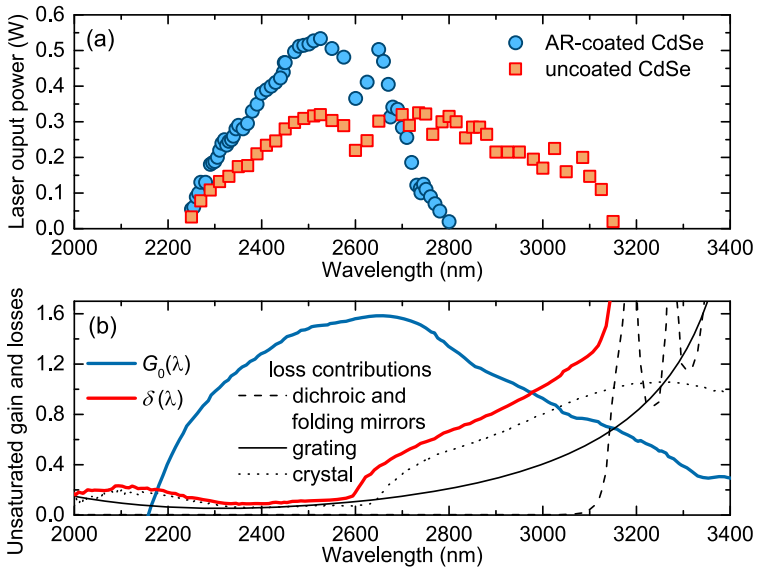

Fig. 6. (a) Emission wavelength tunability of the Cr:CdSe laser for an incident pump power of 1.5 W. (b) Corresponding unsaturated gain (blue curve) and estimated intracavity losses (red curve). Grey dashed, solid, and dotted lines refer to dichroic and folding mirrors, grating, and crystal loss contributions, respectively.

y-axis versus the propagation distance (squares and circles), together with the best interpolating functions (red dashed curves). The Cr:CdSe laser beam is characterized by beam quality factors $M_x^2 = 1.1(1)$ and $M_y^2 = 1.0(1)$, which are consistent with a diffraction limited TEM_{00} Gaussian mode.

3.2. *Wavelength tunability in CW operation*

To investigate wavelength tunability of the Cr:CdSe laser, we replaced the plane output coupler with a 300 groves/mm aluminum-coated reflective grating, with nominal 95% efficiency into the first diffracted order (at 2.55 μm for a linear polarization perpendicular to the groves). The grating is used at 22° incidence angle in a Littrow configuration, as sketched in Fig. 4 (b). Figure 6 (a) shows the measured tunability range at 1.5 W incident pump power. A maximum tunability range of 565 nm, from 2240 to 2805 nm, was obtained (corresponding to ~20% of the peak emission wavelength). The laser power drop around 2.6 μm is due to the intracavity water vapor absorption that can be easily mitigated by N_2 cavity purging. With respect to the broad-emission potentiality of Cr:CdSe laser crystal, the main limitations are represented, on the long wavelength side, by the AR coating performance of the CdSe crystal (see Fig. 1 (b)) and, on the short wavelength side, by the edge of the Cr:CdSe gain profile. Figure 6 (b) shows the calculated unsaturated laser spectral gain at 1.5 W pump power together with the intracavity spectral loss contributions due to the reflectivity spectra of mirrors (dichroic and spherical mirrors) and grating, and the transmission spectrum of the AR-coating of the CdSe crystal. The predicted wavelength tunability range, neglecting the effects due to crystal thermal load (reduction of the laser mode profile and of the radiative lifetime), extends from 2.18 to 2.95 μm, in quite good agreement with the experimental values. To overcome the spectral limitation on the long wavelength side due to the crystal AR-coating, we performed the same tunability experiment using an uncoated Cr:CdSe crystal (same dimensions and Cr-doping level). Although the overall efficiency with the uncoated laser crystal was lower than in the previous case (an optical to

Optical Materials EXPRESS

optical efficiency of 34% at 2.65-μm peak emission wavelength was achieved using the 20% output coupler), the laser emission wavelength reached 3.12 μm, being this value again limited by the spectral reflectivity of the dichroic mirror and the grating spectral efficiency.

3.3. Output power scalability and thermal lensing

To investigate the output power scalability a detailed characterization of the thermal loading effects has been carried out. Figure 7 (a) shows the output versus input power characteristics of the Cr:CdSe laser operated in the best condition corresponding to the 20% output coupler, obtained using three different pump focusing lenses (75, 100, and 200 mm focal length), in CW and quasi-CW pumping regimes. In CW regime of operation the input-output curve presents a marked rollover above a maximum useful pump power level of ~2.5 W (corresponding to 2 W absorbed power), with only a slight dependence on the pump beam dimensions; further pump power increase leads eventually to a complete laser shutoff, due to a thermo-optical effects. Figure 8 shows the measured mode spot sizes (radius at $1/e^2$ of the peak intensity) as a function of the absorbed pump intensity, along with the computed results obtained by a FEA analysis of the resonator [19], taking into account both temperature- and stress-dependent variations of the crystal refractive index. It can be seen that there is a fairly good agreement between experimental data and FEA results. Owing to the low thermal conductivity and the high value of the temperature dependence of refractive index, thermal lensing is indeed very strong, giving rise to an equivalent focal length which varies from ~20 mm near threshold to ~1 mm when the laser is operated at the maximum useful pump power, as calculated by the FEA routine. FEA analysis predicts that, even by increasing the pump power well above the maximum useful level of 2.1 W, the resonator remains within the stability region (the spot-size on the output mirror does not diverge, see dashed lines in Fig. 8). In fact, the position of the crystal adjacent to the dichroic mirror, *i.e.* at a distance from the folding mirror approximately equal to the focal length of the mirror itself, greatly reduces the effects of thermal lensing on the resonator stability, allowing in principle a wide range of usable pump powers, *i.e.* a wide range

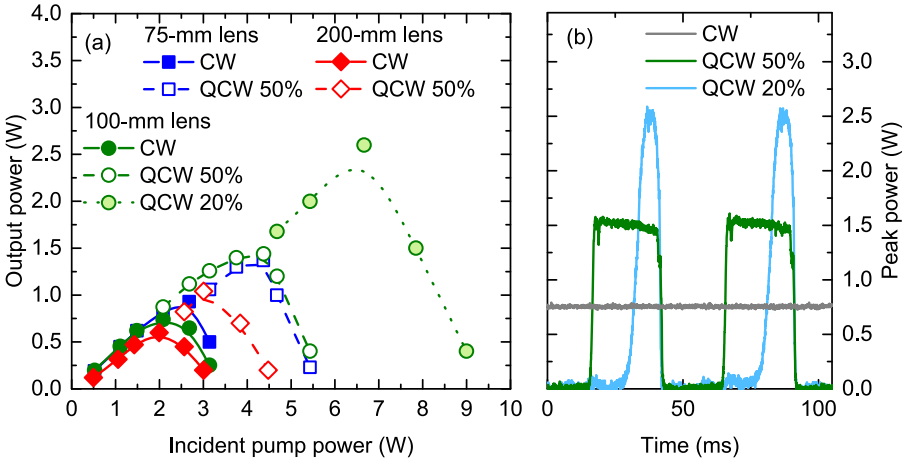

Fig. 7. (a) Output versus input power characteristics of the Cr:CdSe laser with 20% output coupler for three different pump focusing lenses with focal length of 75 mm (squares), 100 mm (circles), and 200 mm (rombs) in CW and quasi-CW pumping regime. (b) Temporal traces of the output power under comparable average thermal loading (2 W average pump power) in CW and quasi-CW (20 Hz with 50% and 20% duty cycle) operating regimes.

Optical Materials EXPRESS

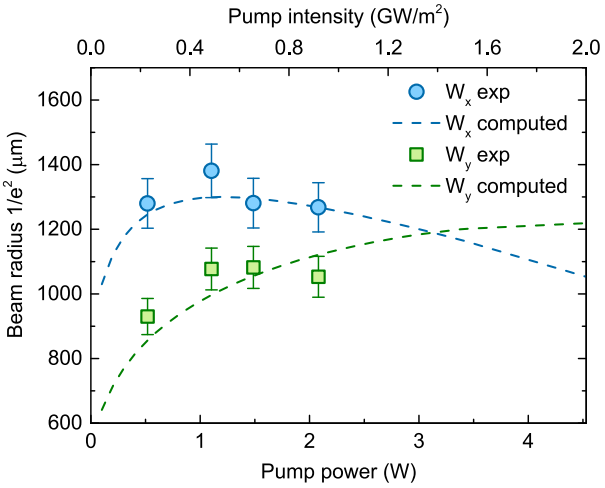

Fig. 8. Laser mode spot sizes ($1/e^2$ intensity radius) measured along the horizontal (x-axis) and vertical (y-axis) planes at the output coupler in CW operation, as a function of absorbed pump intensity (75-mm focal length of the focusing pump lens; 20% output coupler). The dashed lines represent the computed values of the spot sizes obtained by FEA analysis of the resonator (the distance between dichroic and folding mirrors is equal to 50.7 mm).

of dynamic resonator stability. Output power decrease and eventually laser shutoff are therefore mainly ascribable to phase-front distortion of the laser mode inside the thermally loaded crystal, together with a temperature-induced reduction of the upper laser level lifetime. In the same optical configuration, by replacing the Cr:CdSe crystal with a commercial AR-coated Cr:ZnSe crystal (featuring the same pump absorption level), the upper acceptable limit for the pump power readily increased to 18 W, in very good agreement with the results reported in [23]; this much better performance is clearly related to the superior thermo-optical properties of ZnSe crystal as compared with CdSe (see Table 1).

The temperature buildup and thus the thermal loading effects can be partially mitigated operating the laser in a quasi-CW regime. Figure 7 (b) shows a comparison of temporal traces of the output power in CW and quasi-CW regimes at approximately the same average thermal load on the crystal; in all cases a 100-mm focal length lens was used to focus the pump beam inside the crystal. The gray trace refers to pure CW operation at the pump power limit of 2.1 W, corresponding to ~1 W output power. By chopping the pump beam at 20 Hz with 50% duty cycle (25 ms time interval between pulses) the pump power upper limit before rollover becomes ~4 W and further increases to ~7 W when reducing the duty cycle to 25% (40 ms between pump pulses). In these conditions the peak output power raises to 1.5 and 2.5 W, respectively, owing to the temperature decay during the switch-off time of the pump beam. However, the much lower thermal conductivity of CdSe and hence its considerably long thermal relaxation time hamper this effect, greatly reducing its benefit with respect to the results obtained in [23] with a ZnSe crystal.

Finally, it is worth pointing out that no thermal damage of the crystal and AR coatings was observed up to an incident pump power of 10 W, corresponding to an incident intensity of the pump beam of 4 GWm^{-2}.

Optical Materials EXPRESS

4. Conclusion

In conclusion, we have thoroughly characterized the laser performance of a Tm-fiber-laser-pumped Cr:CdSe laser crystal as an efficient and broadly tunable laser source in the mid-IR spectral region. Using an antireflection coated Cr:CdSe crystal we demonstrated diffraction-limited 1-W level pure-CW laser action at around 2.65 μm with 50% slope efficiency (63% against the absorbed pump power), which is the highest so far obtained. Higher output peak power levels up to 2.5 W were achieved in a quasi-CW pump configuration with a repetition frequency of 20 Hz and a duty cycle of 20%. A simultaneous rapid transverse scan of the coaxial laser mode and pump beam across the gain element could be adopted to further increase the output power level, as already demonstrated in [23]. Concerning wavelength tunability, a maximum 0.9-μm tuning range, from 2.2 to 3.1 μm, was obtained using an uncoated Cr:CdSe laser crystal (limited only by the spectral properties of the laser cavity components). These favorable results prove the Cr-doped CdSe laser as an interesting ultra-broadband middle-infrared solid-state source with potential applications in high-resolution molecular spectroscopy, optical frequency standards and metrology, as well as Lidar and Dial systems for atmospheric remote sensing.

Funding

Politecnico di Milano International Fellowship (T. T. Fernandez); Russian Science Foundation research project project 17-79-20431; State Task of the Ministry of Education and Science of the Russian Federation No 3.5267.2017/8.9; Italian Ministry of University and Research (MIUR) and ELI Nuclear Physics (ELI-NP).

Acknowledgments

The authors acknowledge Carlo Brambilla of Politecnico di Milano for the development of the copper crystal support and also thank Vacuum Technology Laboratory LTD Serpukhov, Moscow Region, for AR-coating of Cr^{2+}:CdSe crystal. V. A. L. and M. K. T. acknowledge the Russian Science Foundation according to the research project No. 17-79-20431 for the support of experimental work with mid-IR laser. V. E. K. acknowledges the State Task of the Ministry of Education and Science of the Russian Federation No 3.5267.2017/8.9 for the support of numerical calculations of AR-coating and laser parameters.